ORNL
MASTER COPY

OAK RIDGE NATIONAL LABORATORY
operated by
UNION CARBIDE CORPORATION • NUCLEAR DIVISION
for the
U. S. ATOMIC ENERGY COMMISSION

JUL 7 - 1971

ORNL - TM - 3384

PERFORMANCE OF SPHERE-PAC AND PELLETIZED $(U,Pu)O_2$ DURING SEVERE OVERPOWER TRANSIENTS

C. M. Cox, D. R. Cuneo, and E. J. Manthos

NOTICE This document contains information of a preliminary nature and was prepared primarily for internal use at the Oak Ridge National Laboratory. It is subject to revision or correction and therefore does not represent a final report.

This report was prepared as an account of work sponsored by the United States Government. Neither the United States nor the United States Atomic Energy Commission, nor any of their employees, nor any of their contractors, subcontractors, or their employees, makes any warranty, express or implied, or assumes any legal liability or responsibility for the accuracy, completeness or usefulness of any information, apparatus, product or process disclosed, or represents that its use would not infringe privately owned rights.

ORNL-TM-3384

Contract No. W-7405-eng-26
METALS AND CERAMICS DIVISION

PERFORMANCE OF SPHERE-PAC AND PELLETIZED $(U,Pu)O_2$ DURING SEVERE OVERPOWER TRANSIENTS

C. M. Cox, D. R. Cuneo, and E. J. Manthos

Paper
Presented
at the
Conference on
Fast Reactor Fuel Element Technology
April 13–15, 1971
Materials Science and Technology Division
American Nuclear Society

JULY 1971

OAK RIDGE NATIONAL LABORATORY
Oak Ridge, Tennessee
operated by
Union Carbide Corporation
for the
U.S. ATOMIC ENERGY COMMISSION

CONTENTS

Abstract 1
Introduction 2
Fabrication Data 3
Transient Data 3
Power Distribution 5
Thermal Analysis 10
Postirradiation Examination 16
Conclusions 21
Acknowledgments 25
References 26

PERFORMANCE OF SPHERE-PAC AND PELLETIZED $(U,Pu)O_2$ DURING SEVERE OVERPOWER TRANSIENTS*

C. M. Cox, D. R. Cuneo, E. J. Manthos

ABSTRACT

Six fuel pins containing unirradiated sol-gel-derived $(U,Pu)O_2$ were subjected to power transients at the Transient Reactor Test Facility (TREAT). No failure occurred even though 50 vol % of the fuel melted in the peak power regions of two Sphere-Pac pins.

Although the fuel pins showed no significant dimensional changes, neutron radiographic and destructive examinations showed extensive fuel relocation within the cladding. This included fuel column separations, fuel densification during cooling from a molten state, and axial migration of fuel and perhaps of large bubbles of adsorbed gases in the molten fuel. There was evidence that a gap formed between the Sphere-Pac fuel and cladding by a combination of sintering and shrinkage during cooling from the melt.

The influence of fuel column separations on length changes tended to be offset by sintering and shrinkage. Pellet fuel pins showed occasional separations at pellet interfaces, apparently due to a ratchetting mechanism.

Comparison with data reported by other investigators indicates that, for the types of transients considered in this work, there is no difference between the performance of pellet or Sphere-Pac fuel of the same smear density and sol-gel and coprecipitated pellets behave equivalently.

INTRODUCTION

Understanding the behavior of fuel pins under transient operating conditions is important in evaluating the overpower allowance of fuel element designs, in predicting the influence of temporary abnormal conditions on future pin lifetime and safety margin, and in predicting the initial consequences of pin failures. There is no facility at which the temperature or power transients hypothesized for LMFBR accidents can be imposed on a $(U,Pu)O_2$ fuel pin operating at typical steady state conditions. However, transients from zero power typical of a major control rod ejection accident[1] can be reasonably well simulated in the Transient Reactor Test Facility (TREAT).[2]

This paper describes the results of a series of experiments aimed at comparing the behavior of unirradiated sol-gel-derived $(U,Pu)O_2$ Sphere-Pac and pellet fuel pins during severe power transients causing various amounts of fuel melting. Earlier work by Hanson, Field, Rabin, and Thomas[3–6] indicated that, if no part of the fuel melts in a TREAT-type transient, a previously unirradiated liquid-metal-cooled $(U,Pu)O_2$ fuel pin will not fail. However, considerable axial fuel movement occurs when a significant fraction of the fuel is heated above the melting point.

The principal test variables were fuel smear density, 81 and 88% of theoretical, and fuel fabrication form, pellets and vibratorily compacted microspheres (Sphere-Pac Process).[7] Data reported by Thomas and Field[8] indicate that fuel fabrication form may be a significant variable and that unirradiated Vi-Pac (vibratorily compacted irregular particles) fuel pins may fail from less severe transients than pellet fuel pins of

the same smear density. Other variables that have been shown or are anticipated to influence the transient behavior of mixed oxide fuel pins include transient shape and severity, fuel pin transient temperature distribution, amount of axial restraint, cooling mechanism, axial variations in temperature and power distribution, fuel pin defects, and previous irradiation history.

FABRICATION DATA

The transient tests were conducted with two capsules, each containing three fuel pins in tandem. The fuel pins were encapsulated in stagnant sodium-filled capsules similar in design to those used by Hanson et al.[3] The capsules contained electrical heaters, to heat the fuel pins to approximately 430°C before the transients, and thermocouples adjacent to the fuel pins and at various radial positions in the capsules at the fuel column midplanes.

Each fuel pin had an 8-in.-long fuel column and was clad with 0.254-in. OD × 0.016-in.-wall type 304 stainless steel tubing. The fuel columns were partially restrained axially with a spring-loaded extensometer, which allowed up to 3/16 in. fuel length increase. Fabrication data for the fuel pins are summarized in Table I.

TRANSIENT DATA

The first capsule, TR-1, was initially subjected to a calibration transient to verify the design performance by comparing calculated and measured temperatures in the sodium annulus around the fuel pins. The calculated maximum fuel center-line temperature was about 1800°C for

Table I. Fabrication Data for ORNL TREAT Capsules

	Fuel Pin					
	TR-1A	TR-1B	TR-1C	TR-2A	TR-2B	TR-2C
Fuel fabrication form[a]	P	S	P	S	S	P
U/(U + Pu)[b]	0.801	0.801	0.801	0.801	0.801	0.801
O/(U + Pu)	1.983	1.980	1.991	1.980	1.980	1.990
Gas release, cm^3/g (STP) at 1600°C	0.07	0.14	0.23	0.14	0.14	0.19
Fuel smear density, %TD	88.9	80.9	79.7	82.0	80.9	80.2
Fuel length, in.	8.03	8.00	7.98	8.01	8.00	8.10
Fuel-cladding diametral gap, mils	5		5			5
Gas plenum volume,[c] cm^3	1.1	1.3	1.5	1.3	1.3	1.4

[a]P = solid pellets; S = Sphere-Pac.

[b]Natural U.

[c]Including all porosity.

this calibration transient. The test transients were designed to melt approximately one-fourth of the fuel in the peak power region of the first capsule and half for the second capsule, TR-2. Earlier experiments indicated that failures of previously unirradiated fuel pins should be anticipated with TREAT transients that cause more than 70% of the fuel to melt in pellet fuel pins,[3–6] or that cause 50 to 60% of the fuel to melt in vibratorily-compacted powder fuel pins.[8]

Table II summarizes the TREAT reactor operating data. Note that for the two test transients, 1294 and 1295, the peak reactor power was equivalent, but the energy input to the fuel pins was varied by clipping the transients. The time variation of the heat rate for each of the fuel pins, based on postirradiation burnup analyses and the reactor power history, is shown in Fig. 1.

POWER DISTRIBUTION

The thermal neutron energy spectrum of the graphite-moderated TREAT reactor caused appreciable distortions in both the axial and radial flux profiles. The axial power profiles were measured by the ^{60}Co activity in flux wires located within the capsule near the fuel pins, as shown in Fig. 2. The radial power distributions shown in Fig. 3 were estimated by a 36-group neutron transport theory calculation using the ANISN[9] computer code. The steep radial power profile shown leads to some distortion in the transient temperature distribution in the fuel pins as compared to that in a fast reactor spectrum. However, an earlier detailed analysis of boron, cadmium, and europium neutron filters indicated that significant flattening of the power and temperature profiles was impossible without

Table II. Reactor Data for ORNL TREAT Capsules

	Capsule		
	TR-1	TR-1	TR-2
TREAT transient	1293	1294	1295
Date	10-29-69	10-30-69	10-31-69
Initial reactor period, msec	630	204	200
Peak reactor Power, MW	29.8	202	202
Integrated reactor power, MWsec	88	140	172
Pulse width at half max power, sec	3.6	0.78	0.85
Type transient	clipped	clipped	clipped

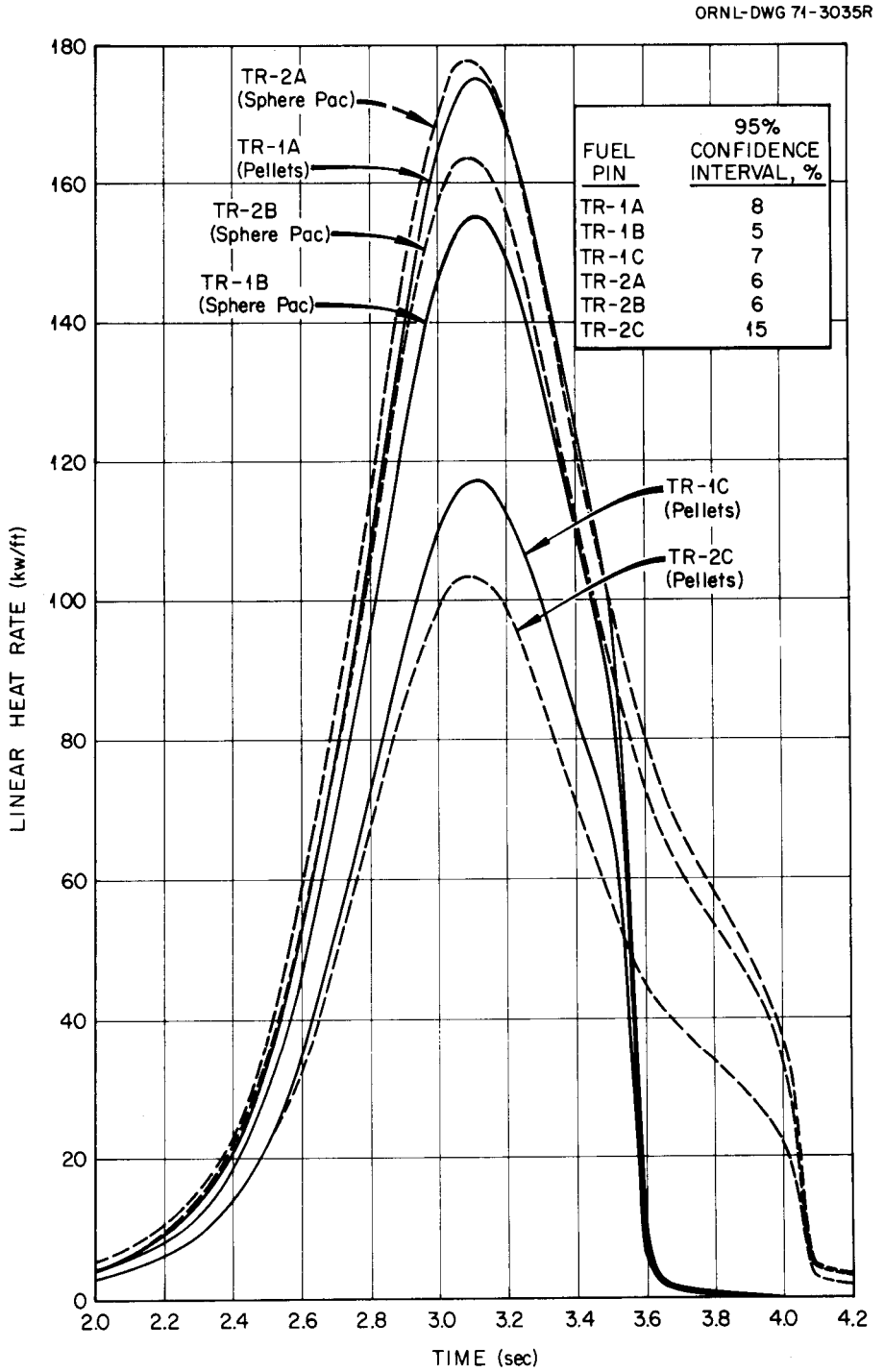

Fig. 1. Time Variation of Heat Rate at Fuel Column Midplanes.

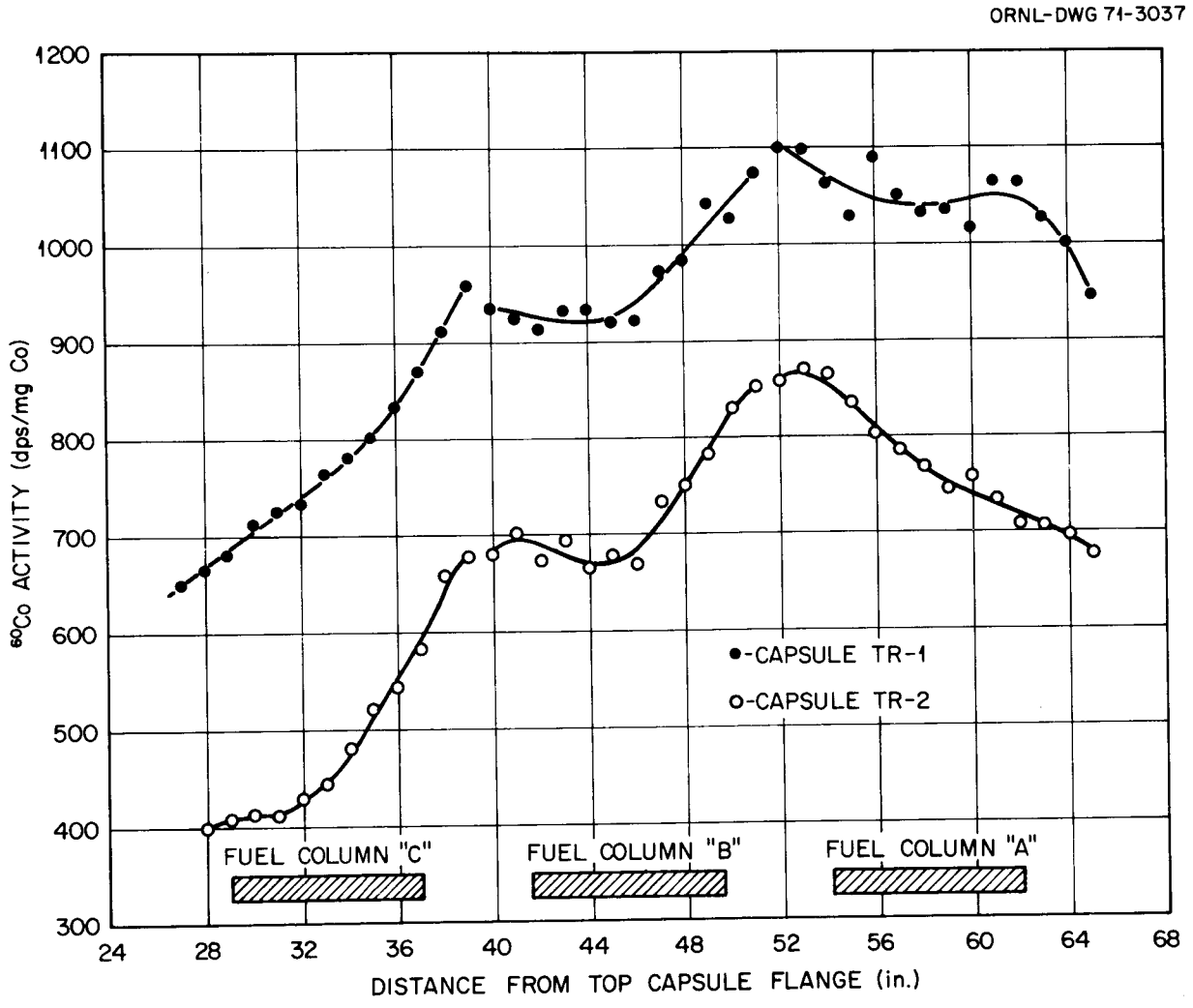

Fig. 2. Activity of Interior Flux Monitor Wires.

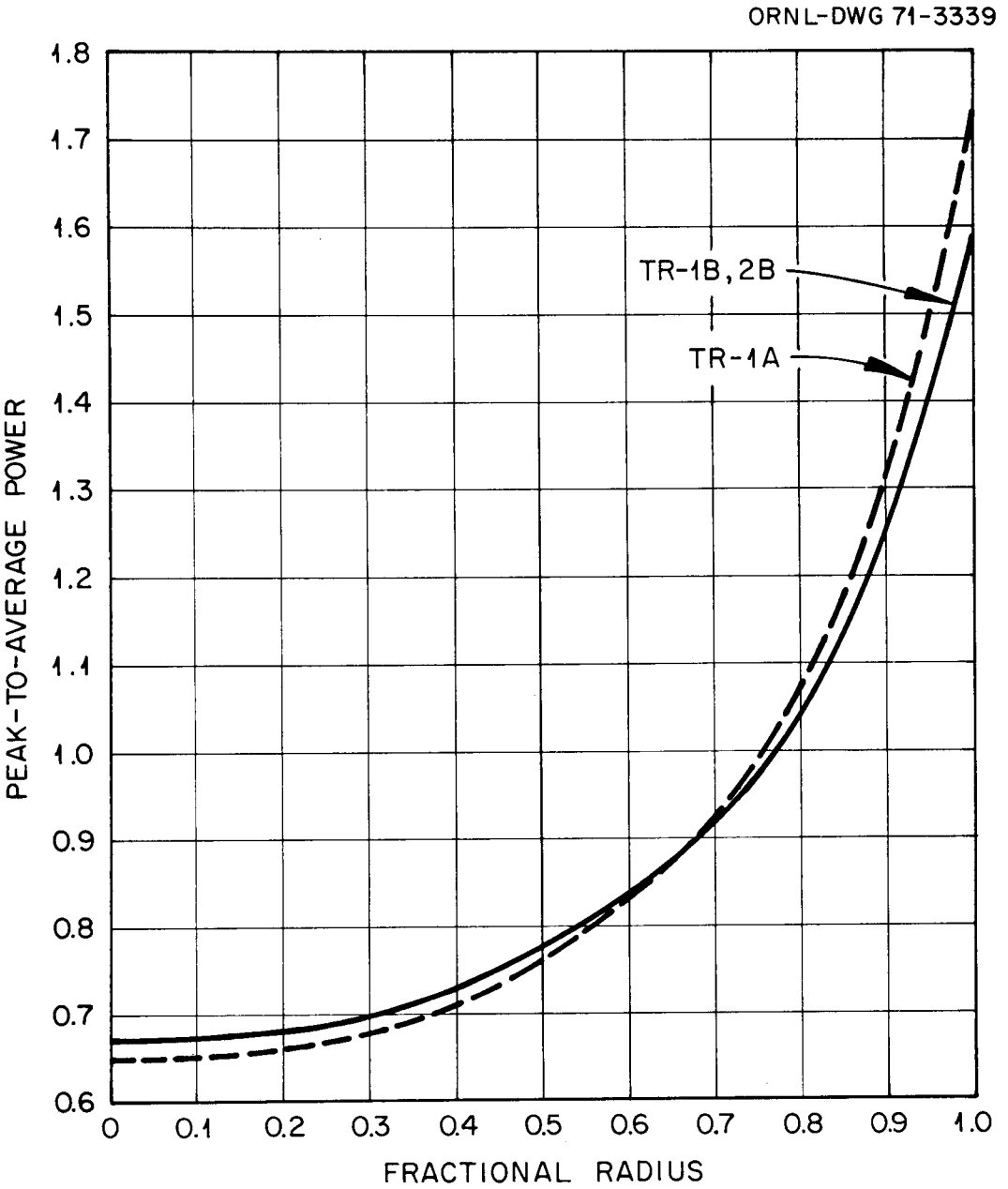

Fig. 3. Radial Power Distribution in Fuel Pins.

decreasing the specimen power intolerably,[10–12] and we must thus accept this atypical feature of the test. The relative power distributions were converted to absolute values based on radiochemical burnup analyses and flux monitor data summarized in Table III. With the exception of fuel pin TR-2C, where the data were discarded because the radiochemical solutions were contaminated, the statistical accuracy of the analyses was excellent. The resulting axial variations in fuel pin linear heat rate, per watt of reactor power, are shown in Fig. 4.

THERMAL ANALYSIS

The thermocouple data obtained during the transient were compared extensively with transient heat transfer calculations, first as a check on the heat transfer model, and second in an attempt to derive some information about the fuel–cladding heat transfer coefficients during the transients. Figure 5 compares calculated and measured temperatures in the sodium annuli at the midplane of Sphere-Pac pin 2B. In this case the calculated temperatures were obtained from the HEATING-3 computer code[13] using temperature-dependent physical properties, including a three-zone temperature-dependent density for the fuel in which the fuel was assumed to densify to 92% of theoretical above 1500°C and 100% above 1900°C. The mixed oxide thermal conductivity was assumed to be represented by the General Electric Company's correlation[14] for temperatures up to the fuel melting point of 2800°C and at higher temperatures was assumed to be approximately half the thermal conductivity predicted by this correlation. The heat capacity and heat of fusion of the oxide fuel were taken from Los Alamos Scientific Laboratory data,[15–16] but

Table III. Burnup Data for Fuel Pins Irradiated in Transient Reactor Test Facility

Fuel Pin	Burnup, as Determined From Indicated Radionuclides, % FIMA[a]							
	^{95}Zr	^{106}Ru	^{141}Ce	^{103}Ru	^{60}Co (interior)	^{60}Co (exterior)	Mean	95% Confidence Interval
	$\times 10^{-6}$	$\times 10^{-6}$	$\times 10^{-6}$	$\times 10^{-6}$	$\times 10^{-6}$	$\times 10^{-6}$	$\times 10^{-6}$	$\times 10^{-6}$
TR-1A					4.36	3.95	4.15	±0.34
TR-1B	3.54	3.59	4.30	4.60	4.24	4.26	4.09	±0.21
TR-1C	2.60	3.04	2.65	4.02	3.43	3.12	3.14	±0.21
TR-2A	2.59	3.12	3.53	3.68	3.39	3.47	3.30	±0.21
TR-2B	2.65	3.00	3.57	4.25	3.17	3.42	3.34	±0.21
TR-2C					2.21	2.32	2.26	±0.34

[a]FIMA = fissions per initial metal atom.

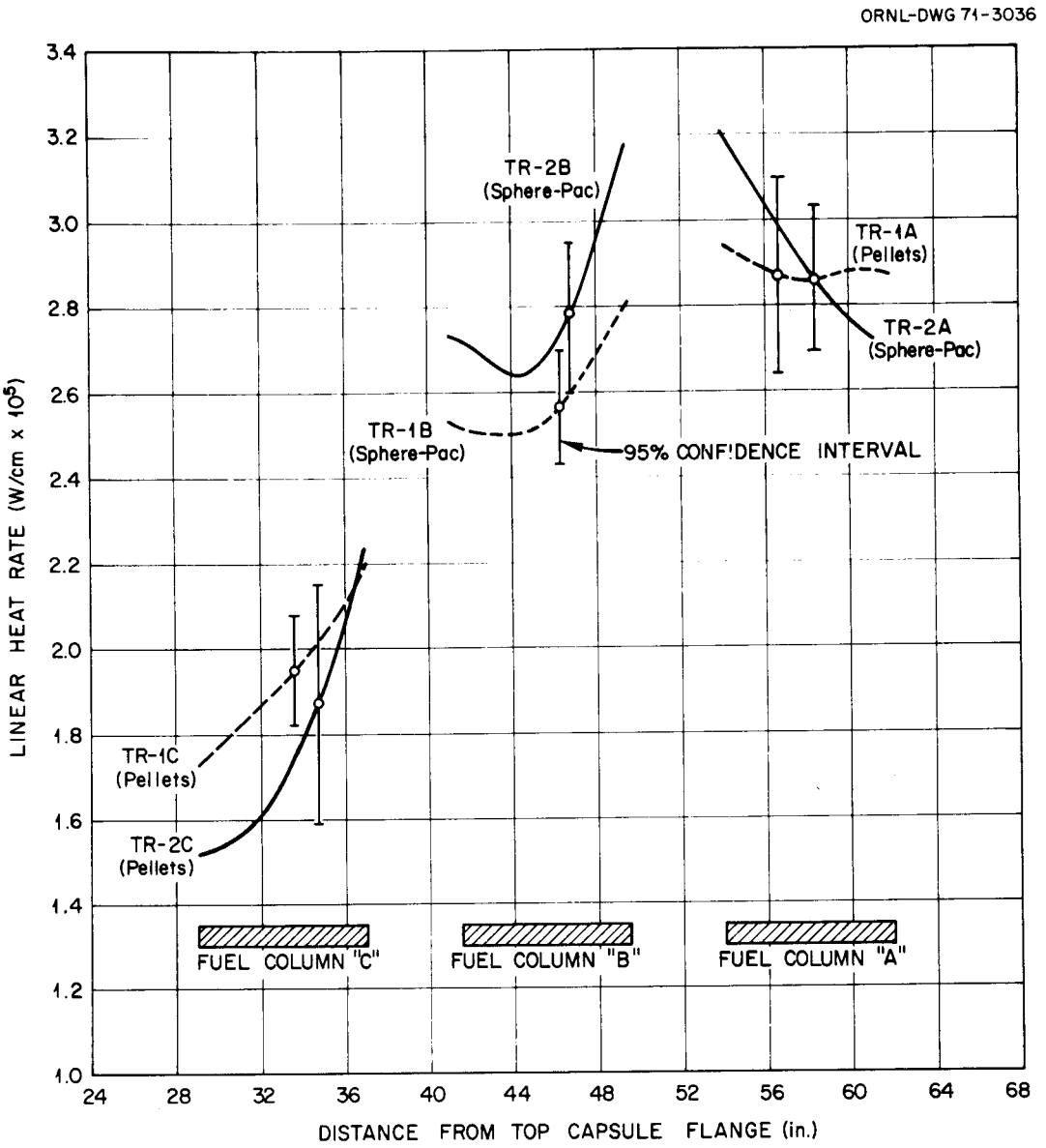

Fig. 4. Linear Heat Rates at 1 W Reactor Power.

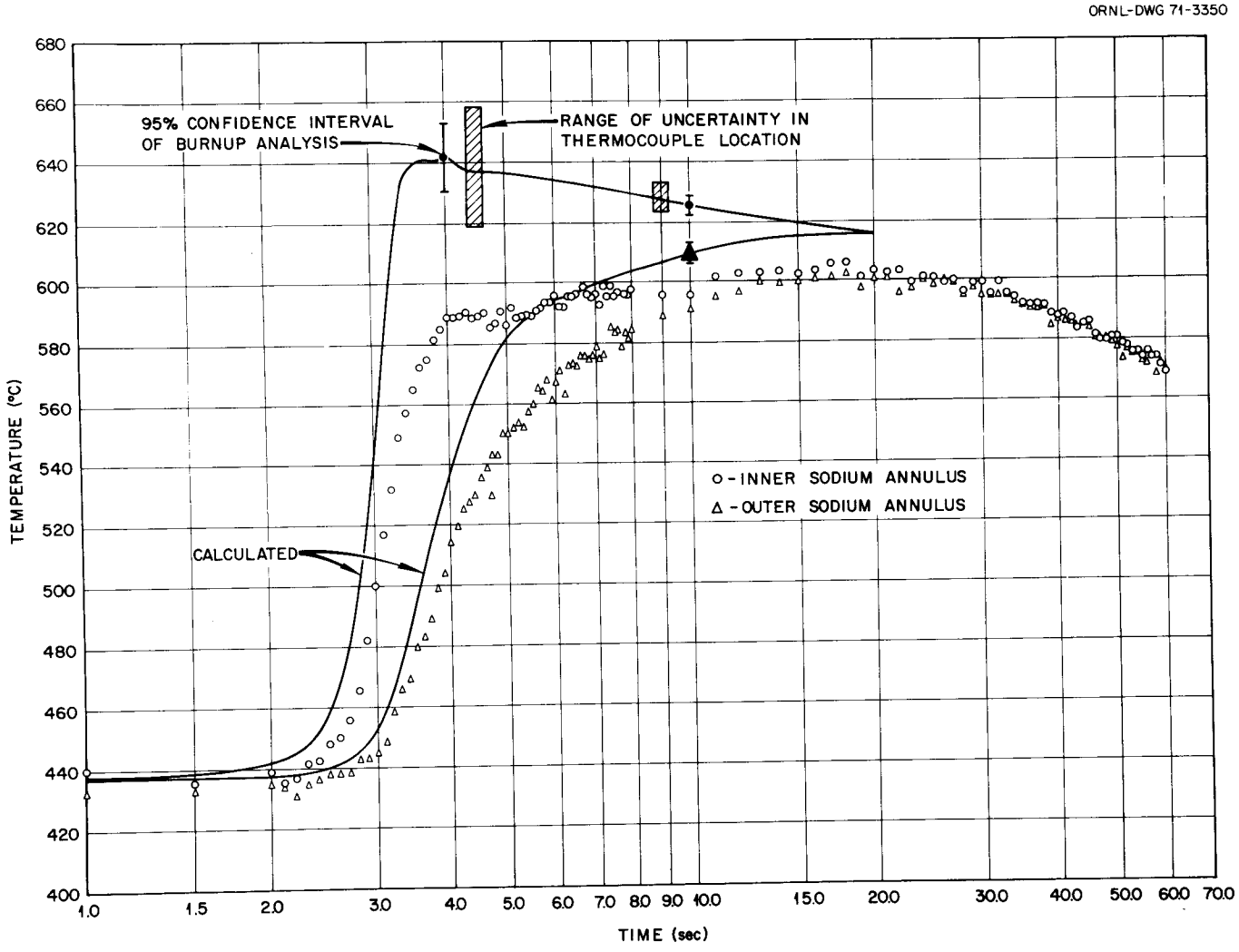

Fig. 5. Comparison of Calculated and Measured Temperatures at Midplane of Sphere-Pac Pin TR-2B.

the former was assumed to be constant at 0.42 J g^{-1} $(°C)^{-1}$ for temperatures above the fuel liquidus, assumed to be 2832°C. The discrepancy between the calculated and measured temperatures in Fig. 5 which range from about 6 to 10% difference, does not appear to follow from either the uncertainty in the burnup analysis or the uncertainty in the thermocouple locations, and we suspect inaccuracies in our values for the thermal properties of the fuel and axial heat flow effects, which were ignored in this analysis.

The predicted temperatures at the thermocouple locations are rather insensitive to the fuel—cladding heat transfer coefficient, and the calculated curves would be essentially the same in Fig. 5 for heat transfer coefficients ranging from 1 W cm^{-2} $(°C)^{-1}$ to infinity. A forced fit of the measured and calculated temperatures based on adjusting the fuel pin power would require approximately a 30% decrease in power, which does not seem justified by the statistical analysis of the burnup data.

The only physically measurable variable that was appreciably affected by the fuel—cladding heat transfer coefficient was the extent of fuel melting. An attempt to correlate the observed and predicted melt volume with the heat transfer coefficient, assumed constant during the transient, is shown in Fig. 6. This plot indicates that heat transfer coefficients of 3.4 W cm^{-2} $(°C)^{-1}$ or greater give the best fit to the observed melt volume for the assumed fuel physical properties and restructuring model. This would indicate that the heat transfer coefficient during the transient would be at least double the steady-state value previously reported by Fitts[17] for Sphere-Pac fuels. While our analysis cannot accurately predict this coefficient, an increase

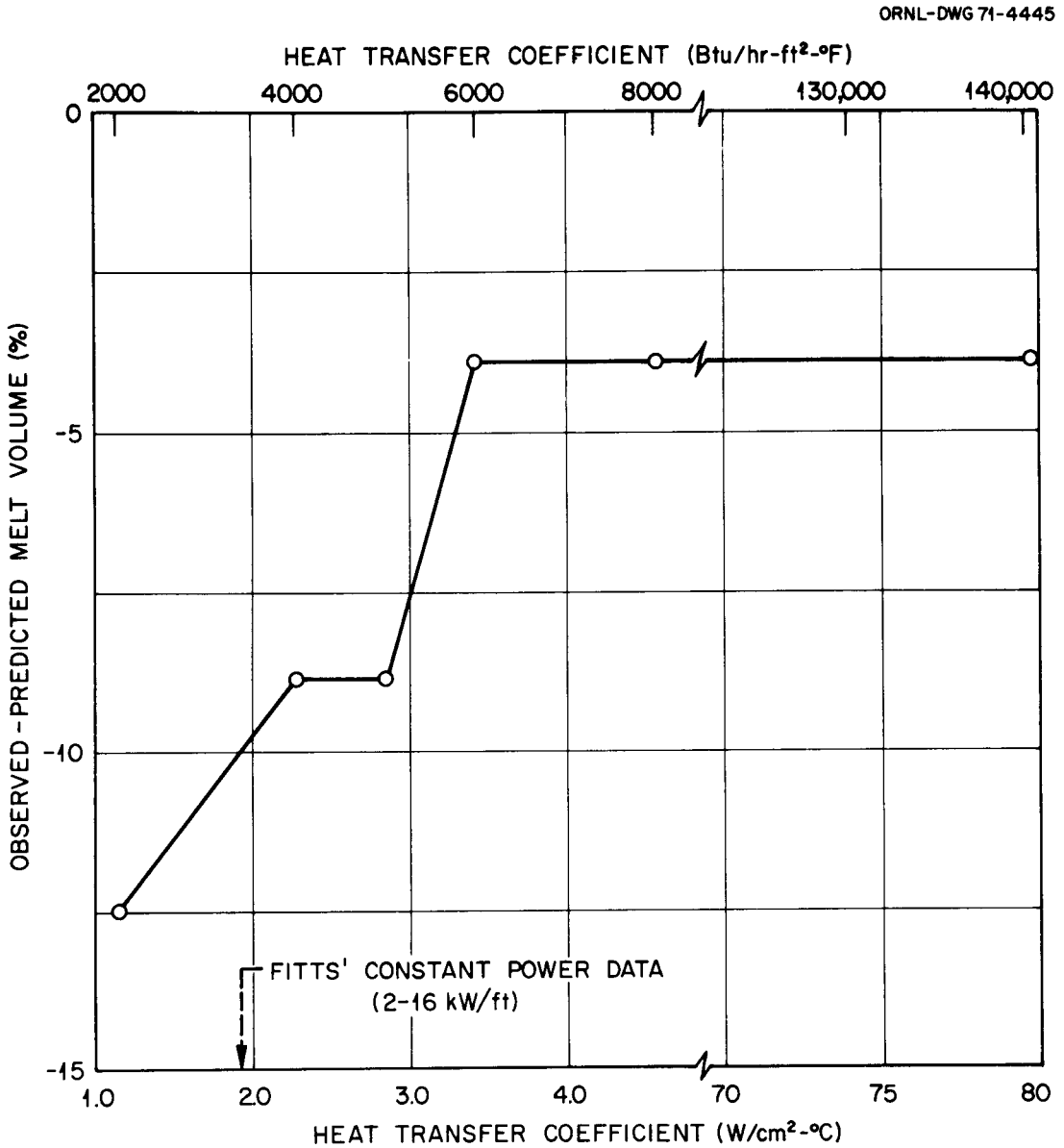

Fig. 6. Correlation of Volume of Molten Fuel with Fuel—Cladding Heat Transfer Coefficient. Sphere-Pac pin TR-2B.

during the transient seems qualitatively correct, since, as shown in Fig. 7, one result of the fuel expansion on melting is to jam the microspheres into the cladding. This micrograph was taken of the fuel—cladding interface in the high-power region of pin 2B. The cladding microstructure shows both localized melting and mechanical deformation.

POSTIRRADIATION EXAMINATION

A postirradiation neutron radiograph of the fuel pins in capsule TR-2, which were subjected to the most severe transient, is shown in Fig. 8. The radiograph, taken at TREAT, indicates fuel column separations, fuel column length changes, and the appearance of a number of chevron-shaped low-density regions. The separations in the pellet fuel pins coincide with pellet interfaces, indicating a ratchetting mechanism. Additional data taken from the neutron radiographs are summarized with other postirradiation data in Table IV. The only measurable dimensional changes to the cladding were regions of slight ovality in the plenum portion of the two top pellet fuel pins. That none of the fuel pins had failed was verified by sampling of the capsule cover gas, detailed visual examinations of the fuel pins, and analysis of the plenum gas.

Figure 9 shows the as-polished microstructure of each of the fuel pins at the fuel column midplane after the transient tests. The large circular voids evident in these photographs are believed to be bubbles formed by coalescence during the high-temperature transients of adsorbed gases present in the fuel from fabrication. The greater amount and larger bubbles in pin 1B as compared to 1A follow from the lower density of the fuel and the higher as-fabricated adsorbed gas content. While

R-54838

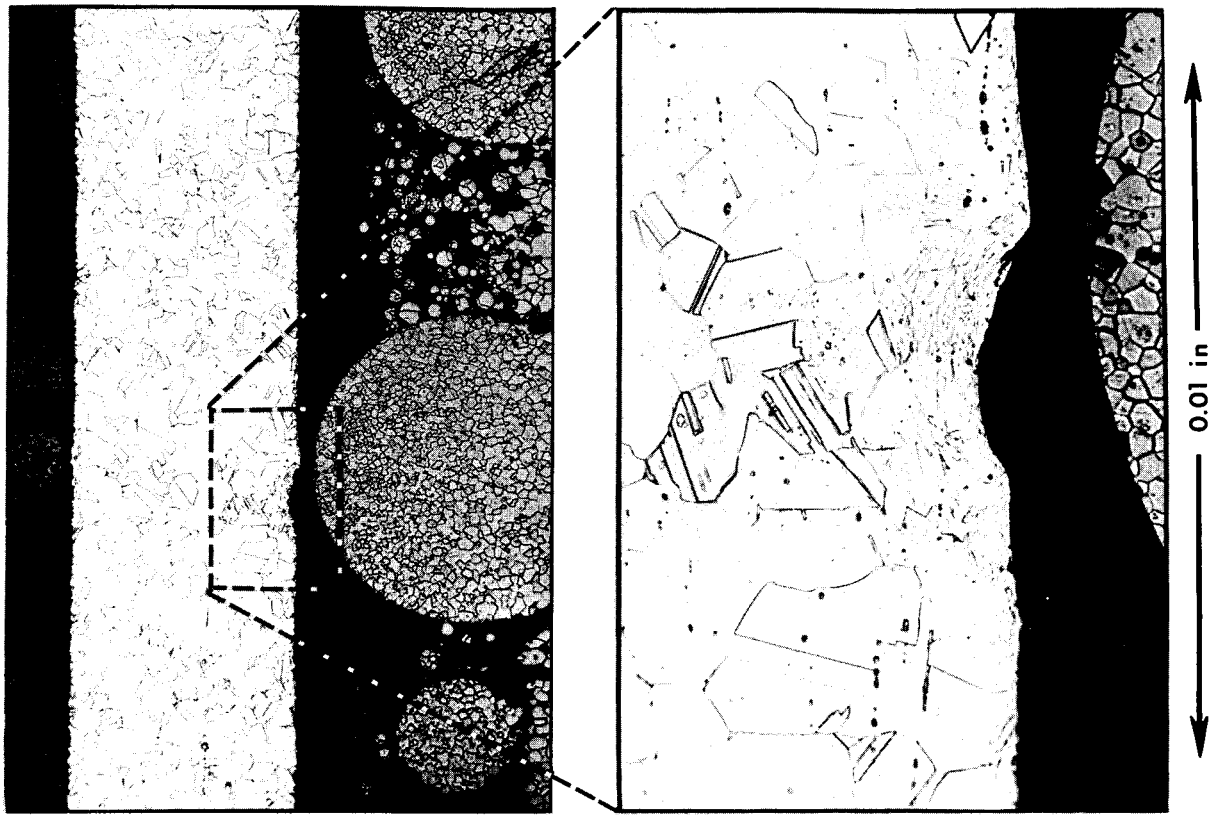

Fig. 7. Point of Contact of Large Microsphere with Cladding During Irradiation.

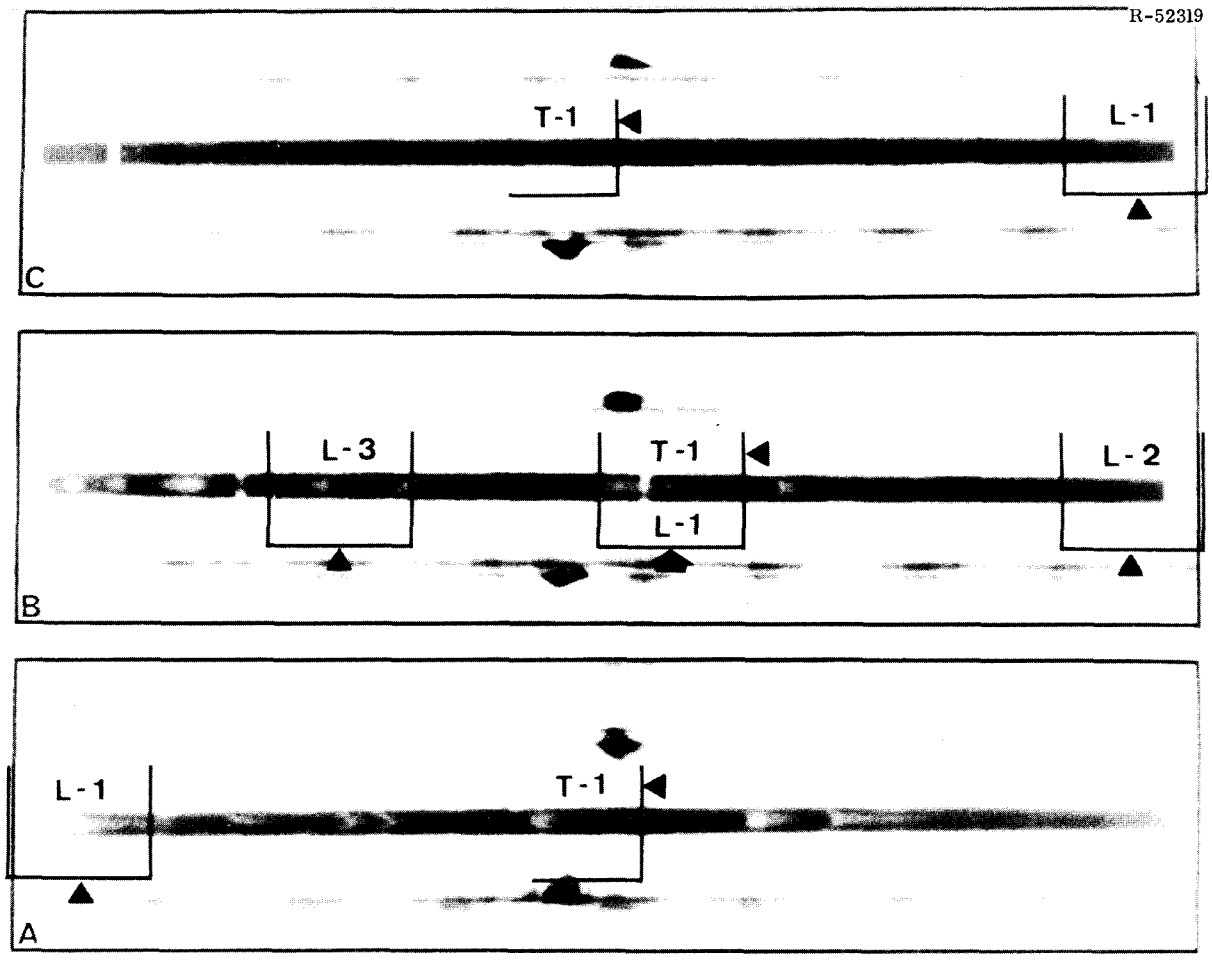

TR-2

Fig. 8. Postirradiation Neutron Radiographs of ORNL TREAT Capsule TR-2.

Table IV. Summary of Operating and Examination Data for ORNL TREAT Capsules

	Fuel Pin					
	TR-1A	TR-1B	TR-1C	TR-2A	TR-2B	TR-2C
Fabrication Data						
Fuel fabrication form[a]	P	S	P	S	S	P
Fuel smear density, % of theoretical	88.9	80.9	79.7	82.0	80.9	80.2
Operating[b]						
Fuel pin temperature before transient,[b] °C	410	449	414	400	436	410
Peak instantaneous linear power,[b] kW/ft	175	155	118	178	164	103
Energy release,[b] cal/g	390	380	292	525	491	313
Postirradiation Examination						
Cladding maximum ovality,[c] max diam − min diam, mils	< 0.5	< 0.5	1.5	< 0.5	< 0.5	1.8
Overall fuel column length change,[d] mils	90	−20	−30	−60	−30	40
Radius of fuel central void,[b] mils	0	0	0	17	28	0
Volume of fuel melting[b]	0	0	0	$50^{\pm 2}$	$51^{\pm 2}$	0
Radius of equiaxed grain growth[b]	94	111	0	111	111	78
Fuel-cladding radial gap,[b] mils	$2.4^{\pm 1.2}$	$3^{\pm 3}$	$1.5^{\pm 1}$	$4.4^{\pm 2.6}$	$3.7^{\pm 3}$	$1.2^{\pm 1.2}$

[a]P = solid pellets; S = Sphere-Pac.

[b]At fuel column midplane.

[c]Maximum diametral increase < 0.5 mil.

[d]Based on neutron radiographs; estimated accuracy ± 20 mils.

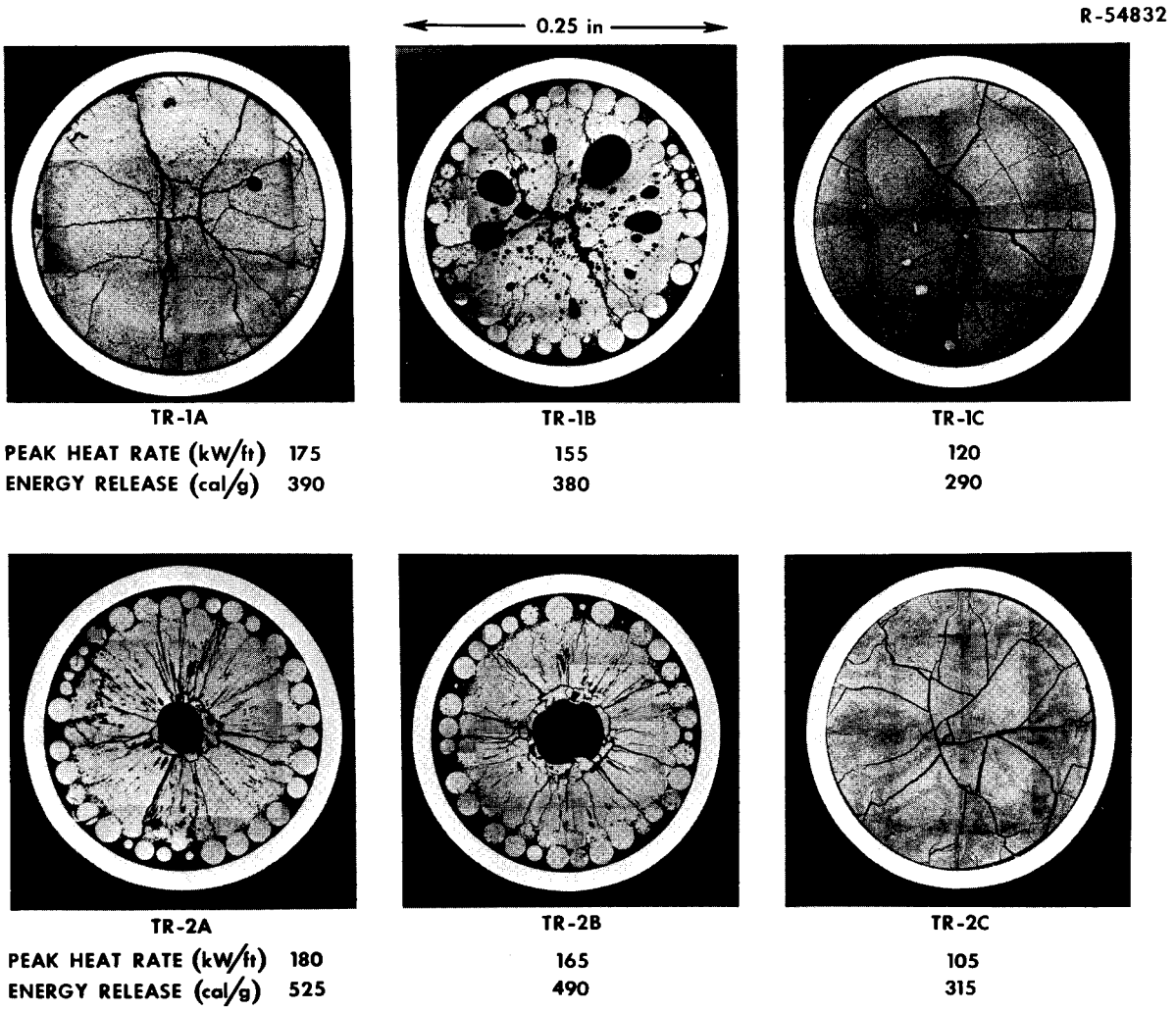

Fig. 9. Transverse Sections Taken from the Midlengths of Fuel Pins Irradiated in TREAT Experiments and Fueled with $U_{0.8}Pu_{0.2}O_{1.98}$.

appreciable restructuring in these two pins was apparent, there was no indication that the fuel had melted except near the ends of the pins, where flux peaking was evident, as shown in Fig. 10. After being etched, the fuel pins were examined for the extent of melting and grain growth, as shown in Fig. 11 for pin 2B. Only the two pins with the highest energy release, 2A and 2B, were identified as having melted at the fuel midplane. It also appears in Fig. 11 that Sphere-Pac fuel, after appreciable densification during the transient, shrank away from the cladding leaving a gap. Failure to obtain the desired 25 vol % fuel melting in the first capsule is attributed to the fact that the amount of fuel melting is extremely sensitive to energy release for fuel melts less than 50 vol %. Appreciable grain growth was observed in all pins but TR-1C, as summarized in Table IV. The chevron-shaped low-density regions observed on the neutron radiographs are shown in Fig. 12 to have been due to the formation of voids as the fuel melted and due to axial relocation of the oxide fuel.

This evidence of fuel pin integrity but appreciable fuel restructuring, fuel cracking, and axial fuel relocation is quite similar to the results of comparable transient tests with unirradiated fuel pins containing coprecipitated $(U,Pu)O_2$ pellets described by Hanson, Field, Rabin, and Thomas.[3–6]

CONCLUSIONS

These experiments have determined that unirradiated sol-gel Sphere-Pac $(U,Pu)O_2$ fuel pins can accommodate severe TREAT-type transients, which cause fuel volume melts up to at least 50%, without failing.

R-54900

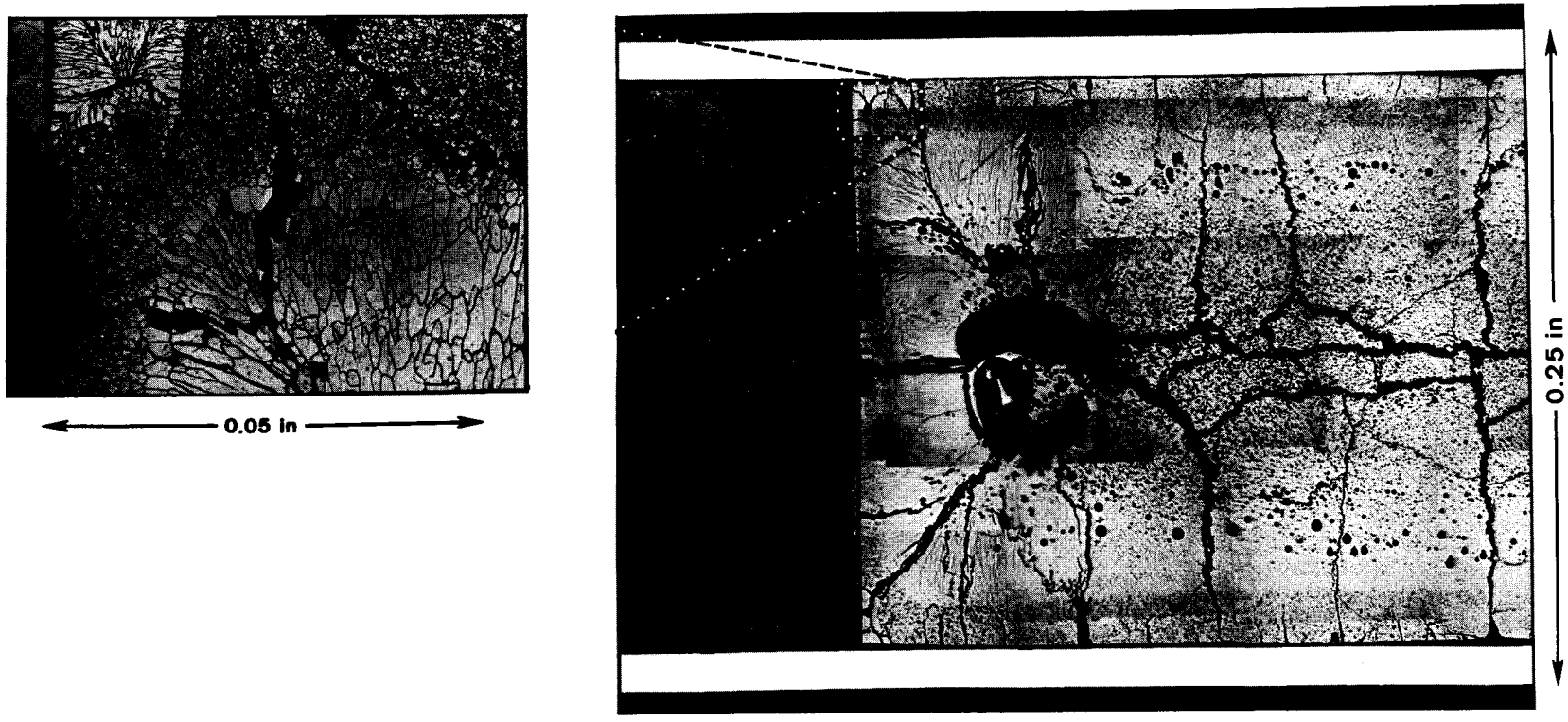

Fig. 10. Effect of Flux Peaking on Fuel Microstructure.

R-53348

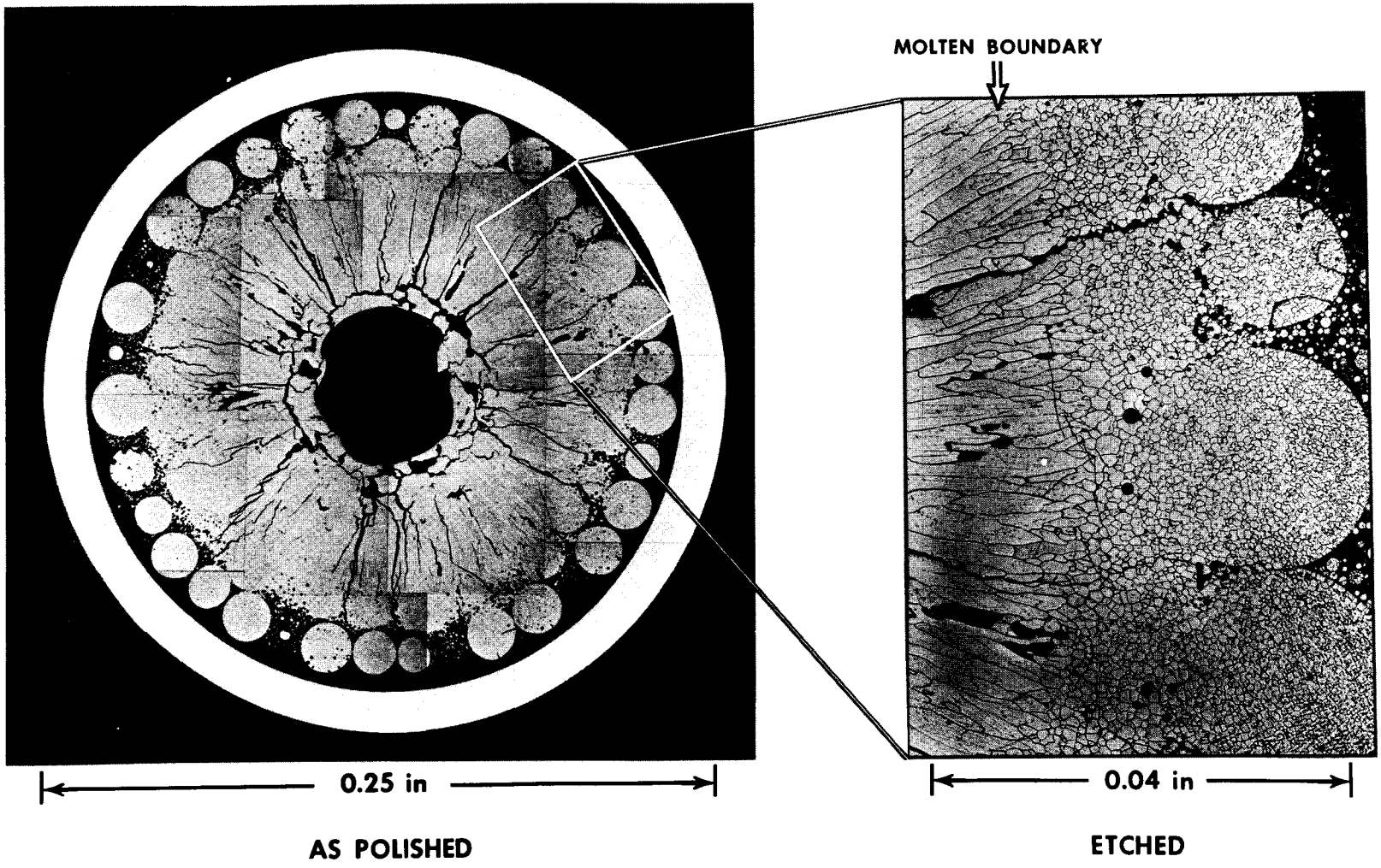

Fig. 11. Location of Melt Radius in Fuel Pin TR-2B.

R-54840

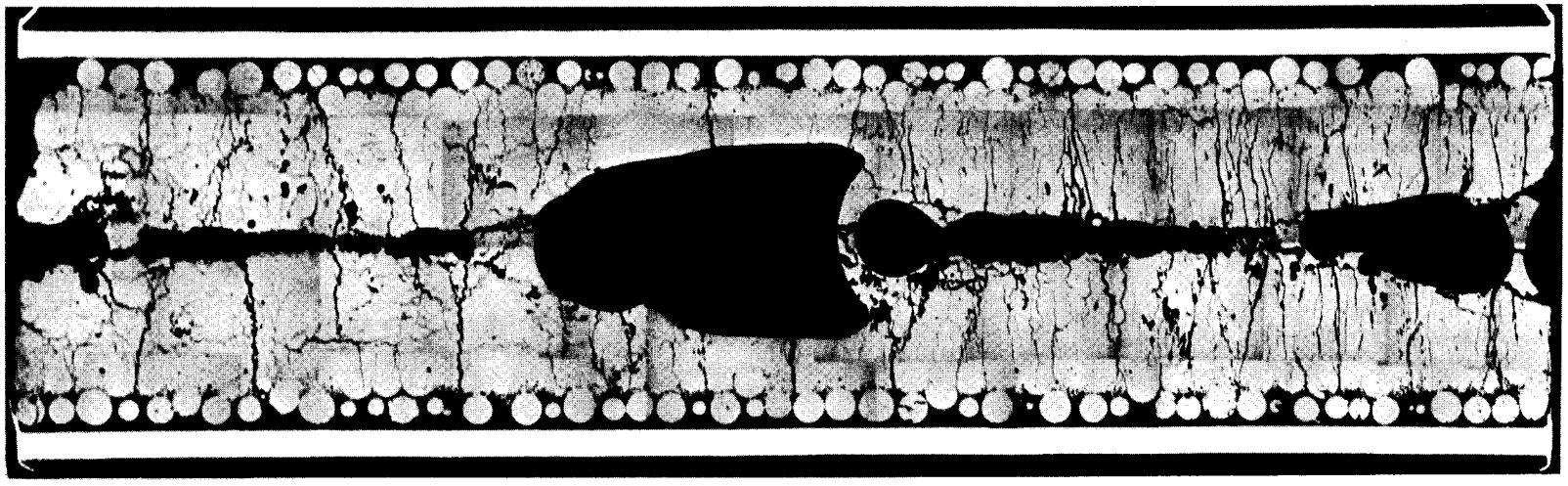

Fig. 12. Gross Restructuring of $U_{0.8}Pu_{0.2}O_{1.98}$ Microsphere Fuel Irradiated at a Peak Heat Rate of 165 kW/ft (TR-2B-1-3).

Although the fuel pins showed no significant dimensional changes, neutron radiographic and destructive examinations found extensive fuel relocation within the cladding. This included fuel column separations, fuel densification as columnar grains formed during cooling from a molten state, and axial propagation of large bubbles formed by coalescence in the molten fuel of adsorbed gases from fabrication. There was evidence that a gap formed between the Sphere-Pac fuel and cladding by a combination of sintering and shrinkage during cooling from the melt.

The influence of fuel column separations on length changes tended to be offset by the same sintering and shrinkage. The pellet fuel pins showed occasional separations at pellet interfaces, apparently due to a ratchetting mechanism.

Comparison with data reported by other investigators indicates that, for the types of transients considered in this work, there is no difference between the performance of pellet or Sphere-Pac fuel of the same smear density and sol-gel and coprecipatated pellets behave equivalently.

ACKNOWLEDGMENTS

The authors gratefully acknowledge the assistance of the following ORNL staff members: E. L. Long, Jr. in metallographic interpretation, J. D. Jenkins in reactor physics analysis, W. D. Turner in heat transfer analysis, and W. J. Lackey in statistical analysis of the burnup data.

REFERENCES

1. W. E. BAILY, Sodium-Cooled Reactors Fast Ceramic Reactor Development Program, Twentieth Quarterly Report, February–April 1969, GEAP-10028 General Electric Company, Breeder Reactor Development Operation, pp. 4-1–4-5.
2. G. A. FRUEND et al., Design Summary Report on the Transient Reactor Test Facility, TREAT, ANL-6034, Argonne National Laboratory (1960).
3. J. E. HANSON, J. H. FIELD, and S. A. RABIN, Experimental Studies of Transient Effects in Fast Reactor Fuels, Series II: Mixed Oxide (PuO_2–UO_2) Irradiations, GEAP-4804, General Electric Company, Advanced Products Operation (1965).
4. J. E. HANSON and J. H. FIELD, "Experimental Studies of Transient Effects in Fast Ceramic Reactor Mixed Oxide (PuO_2–UO_2) Fuels," Trans. Am. Nucl. Soc., 8(1), 42 (1965).
5. G. R. THOMAS and J. H. FIELD, "Response of Axially Restrained Pellet Fuel to Transient Overpower," Trans. Am. Nucl. Soc., 10(2), 707–709 (1967).
6. G. R. THOMAS and J. H. FIELD, "Destructive Examination of an Axially Restrained Pelleted Mixed Oxide Specimen That Failed During Transient Overpower Conditions," Trans. Am. Nucl. Soc., 11(2), 697–698 (1968).
7. F. G. KITTS, R. B. FITTS, and A. R. OLSEN, "Sol-Gel Urania-Plutonia Microsphere Preparation and Fabrication into Fuel Rods," pp. 195–210 in Intern. Symp. Plutonium Fuels Technol., Scottsdale, Ariz., 1967, Nucl. Met. 13, ed. by K. E. Horton, R. E. Macherey, and R. J. Allio, American Institute of Mining, Metallurgical, and Petroleum Engineers, New York (1968).

8. G. R. THOMAS and J. H. FIELD, "Transient Performance of Mixed Oxide Powder Fuel With up to 60% Melting," Trans. Am. Nucl. Soc., 12, 343 (1969).

9. W. W. ENGLE, JR., A Users Manual for ANISN, a One-Dimensional Discrete Ordinates Transport Code with Anisotropic Scattering, K-1693, Oak Ridge Gaseous Diffusion Plant (March 30, 1967).

10. C. E. BREIZY (Comp.), Sodium-Cooled Reactors, Fast Ceramic Reactor Development Program, Sixteenth Quarterly Report for August–October 1965, GEAP-4982, General Electric Company, Advanced Products Operation.

11. C. M. COX and J. D. JENKINS, "Transient Testing of Sol-Gel-Derived $(U,Pu)O_2$," Fuels and Materials Development Program Quart. Progr. Rept. June 30, 1968, ORNL-4330, pp. 23–24.

12. C. M. COX, "Transient Testing of Sol-Gel-Derived $(U,Pu)O_2$," Fuels and Materials Development Program Quart. Rept. Sept. 30, 1968, ORNL-4350, pp. 29–31.

13. W. D. TURNER and M. SIMAN-TOV, HEATING 3 – An IBM 360 Heat Conduction Program, ORNL-TM-3208, Oak Ridge National Laboratory (February 1971).

14. W. E. BAILY et al., "Thermal Conductivity of Uranium-Plutonium Oxide Fuels," pp. 293–308 in Intern. Symp. Plutonium Fuels Technol., Scottsdale, Ariz., 1967, Nucl. Met. 13, ed. by K. E. Horton, R. E. Macherey, and R. J. Allio, American Institute of Mining, Metallurgical, and Petroleum Engineers, New York (1968).

15. J. G. REAVIS and C. W. BAKER, Quarterly Status Report on the Advanced Plutonium Fuels Program for October 1 Through December 31, 1967, LA-3880-MS, Los Alamos Scientific Laboratory p. 19.

16. A. E. OGARD and J. A. LEARY, "High Temperature Heat Content and Heat Capacity of Uranium Dioxide and Uranium Dioxide-Plutonium Dioxide Solid Solutions," pp. 651–655 in Symposium on the Thermodynamics of Nuclear Materials, Vienna, 1967, International Atomic Energy Agency; also published as LA-DC-8620, Los Alamos Scientific Laboratory (1965).

17. R. B. FITTS, E. L. LONG, JR., and J. L MILLER, "Tests of Thermal Performance," Fuels and Materials Development Program Quart. Progr. Rept. Dec. 31, 1970, ORNL-TM-3300, pp. 23–25.

INTERNAL DISTRIBUTION

1–3. Central Research Library
4. ORNL – Y-12 Technical Library Document Reference Section
5–14. Laboratory Records Department
15–134. Laboratory Records (FREP)
135. Laboratory Records, RC
136. ORNL Patent Office
137. R. E. Adams
138. G. M. Adamson, Jr.
139. E. E. Bloom
140. R. A. Bradley
141. J. A. Conlin
142–146. C. M. Cox
147. F. L. Culler, Jr.
148–152. D. R. Cuneo
153. J. E. Cunningham
154. R. B. Fitts
155. B. Fleischer
156. J. H Frye, Jr.
157. W. O. Harms
158–160. M. R. Hill
161. F. J. Homan
162. J. D. Jenkins
163. W. J. Lackey
164. J. M. Leitnaker
165. E. L. Long, Jr.
166. A. L. Lotts
167–171. E. J. Manthos
172. W. R. Martin
173. H. E. McCoy
174. C. J. McHargue
175. A. R. Olsen
176. P. Patriarca
177. W. H. Pechin
178. J. L. Scott
179. J. D. Sease
180. V. J. Tennery
181. D. B. Trauger
182. W. D. Turner
183. T. N. Washburn
184. A. M. Weinberg
185. J. R. Weir, Jr.

EXTERNAL DISTRIBUTION

186. W. E. Baily, General Electric, BRDO, Sunnyvale, CA 94086
187. C. J. Baroch, Babcock & Wilcox, P. O. Box 1260, Lynchburg, VA 24505
188. D. F. Cope, RDT, SSR, AEC, Oak Ridge National Laboratory
189. Jose W. Dias, Graduate Student, 5532 Boelter Hall, UCLA School of Engineering and Applied Science, University of California, Los Angeles, CA 90024
190. C. E. Dickerman, Argonne National Laboratory, 9700 South Cass Ave., Argonne, IL 60439
191. E. A. Evans, WADCO, P. O. Box 1970, Richland, WA 99352
192. J. Green, Los Alamos Scientific Laboratory, P. O. Box 1663, Los Alamos, NM 87544
193. T. Iltis, RDT, SSR, AEC, Westinghouse, ARD, P. O. Box 154, Madison, PA 15663
194. D. L. Keller, Battelle Memorial Institute, 505 King Ave., Columbus, OH 43201
195. E. E. Kintner, RDT, AEC, Washington, DC 20545
196. P. J. Levine, Westinghouse, ARD, Waltz Mill Site, P. O. Box 158, Madison, PA 15663
197. C. L. Matthews, RDT, OSR, AEC, Oak Ridge National Laboratory
198. P. Murray, Westinghouse, ARD, Waltz Mill Site, P. O. Box 158, Madison, PA 15663
199. M. V. Nevitt, Argonne National Laboratory, 9700 South Cass Ave., Argonne, IL 60439
200. E. C. Norman, RDT, AEC, Washington, DC 20545

201. H. Pearlman, Atomics International, P. O. Box 309, Canoga Park, CA 91304
202. W. E. Ray, Westinghouse, ARD, Waltz Mill Site, P. O. Box 158, Madison, PA 15663
203. S. Rosen, RDT, AEC, Washington, DC 20545
204. P. G. Shewman, Argonne National Laboratory, 9700 South Cass Ave., Argonne, IL 60439
205. S. Siegel, Atomics International, P. O. Box 309, Canoga Park, CA 91304
206. J. M. Simmons, RDT, AEC, Washington, DC 20546
207. A. A. Strasser, United Nuclear Corp., Grasslands Rd., Elmsford, NY 10523
208. C. E. Weber, RDT, AEC, Washington, DC 20546
209. G. A. Whitlow, Westinghouse, ARD, Waltz Mill Site, P. O. Box 158, Madison, PA 15663
210. Laboratory and University Division, AEC, ORO
211–212. Division of Technical Information Extension
213-215. Director, Division of Reactor Licensing, AEC, Wash.
216-217. Director, Division of Reactor Standards, AEC, Wash.